SIZE EFFECT ON FAILURE OF BOND SPLICES OF STEEL BARS IN CONCRETE BEAMS

By Sıddık Şener,[1] Zdeněk P. Bažant,[2] Fellow, ASCE, and Emilie Becq-Giraudon[3]

ABSTRACT: The results of reduced-scale failure tests of simply supported four-point-bend beams of different sizes, containing lapped bond splices of smooth (undeformed) longitudinal reinforcing bars, are reported. The tests consist of two groups, with splices located either in the midspan region with a uniform bending moment, or in one of the end regions with a uniform shear force. The specimens were made of microconcrete with a maximum aggregate size 4.76 mm. Beams of three different heights (50, 100, and 200 mm) were tested. The beams were geometrically similar in three dimensions, and even the bar diameters and cover thicknesses were scaled in proportion. The reinforcement ratio was 0.31%. The results reveal the existence of a significant size effect, which can be approximately described by the size effect law previously proposed by Bažant. The size effect is found to be stronger for splices without any spiral than for splices confined by a spiral, and stronger for splices in the maximum shear force region of a beam than for splices in the maximum bending moment region. Generalization of the existing formula of Orangun et al. is proposed and recommended for design. Although the formula provides a safer alternative to the existing approach, further testing is needed for better calibration. The size effect on the nominal bond strength implied by the development length provisions of the current and previous American Concrete Institute code is discussed and shown to be inadequate.

INTRODUCTION

Previous studies, reviewed in Bažant and Planas (1998), ACI 446 (''Fracture'' 1992), and Bažant et al. (1994), reveal that brittle failures of reinforced concrete structures generally exhibit a significant size effect, which cannot be described by plastic limit analysis formulas based on the concept of strength. This is at variance with the formulas underlying the specifications in the current American Concrete Institute (ACI) building code ACI 318-95 (''Building'' 1995), which are conceptually based on plastic limit analysis.

Plastic limit analysis requires that, at the moment of failure, the structure reaches a limit state in which it behaves as a mechanism with a single degree of freedom, fails simultaneously at all points of the failure surface, and mobilizes the material strength simultaneously at all of these points. In brittle failures, however, no such limit state exists. The material strength is reached at different points of the failure surface at different times, and the failure propagates along the failure surface. At the maximum load, only a part of the failure surface reaches the strength limit, while other parts have not yet reached the strength limit or are already softening in the post-peak range, or have already completely lost their stress carrying capacity, i.e., they developed a crack (Fig. 1.2.4, Bažant and Planas 1998).

The size effect generally stems from the fact that the larger the structure, the more localized is the zone at which the strength limit is reached (relative to the cross-sectional dimension). This localization is a phenomenon governed by stability and energy release considerations, and is properly handled within the framework of fracture mechanics.

In contrast to plastic limit analysis, fracture mechanics always exhibits a size effect [provided the failure occurs only after a large stable crack growth, as is typical of reinforced concrete (Bažant and Planas 1998)]. The strongest possible size effect is obtained for linear elastic fracture mechanics (LEFM), in which the material failure is considered to happen at any given time only at one point, the crack tip, which propagates across the cross section. In concrete, which is a quasi-brittle material, the material failure occurs in a fracture process zone of a finite size, which is approximately independent of the structure size.

In a larger structure, the fracture process zone occupies a smaller portion of the cross section; i.e., it is more localized. Therefore, the response is closer to that predicted by LEFM, for which the fracture process zone is assumed shrunken to a point. In a small structure—for example, in a laboratory specimen—the fracture process zone occupies a large portion of the cross section, and thus the failure behavior is closer to plastic limit analysis, which means that the strength limit is reached simultaneously in most of the failure surface. Thus, it is clear that the size effect, defined as the dependence of the nominal strength on the structure size for geometrically similar structures, represents a transition from plastic limit analysis at very small sizes to LEFM at very large sizes.

The size effect typical of quasi-brittle failure behavior has been experimentally demonstrated and theoretically justified for the diagonal shear failure of reinforced concrete beams (both without and with stirrups, and both non-prestressed and prestressed), the torsional failure of reinforced concrete beams, the punching shear failure of reinforced slabs, the pullout failure of reinforcing bars embedded in concrete (Bažant and Şener 1988; Bažant et al. 1995); the pullout failure of anchors with studs; the compression punch failure of concrete cylinders; the beam and ring failures of unreinforced pipes; and, for a size range not over 1:10, the Brazilian split-cylinder test (see the extensive literature reviews in ''Fracture'' 1992; Bažant et al. 1994; Bažant and Planas 1998). It has been observed that, in all of these failures, the size effect is consistent with the approximate formula for the size effect law proposed in Bažant (1984), which is explained by energy release due to fracture. Other formulas, e.g., those based on the Weibull theory or fractal concepts (Bažant 1995; Bažant and Planas 1998), also have been suggested for describing the size effect in brittle failures of reinforced concrete; however, they lack a consistent theoretical basis.

The failure of lapped splices of reinforcing bars embedded in concrete is known to be also a quasi-brittle failure. Hence, a size effect must be expected. The existence of a significant size effect on lap splices, albeit weaker than the LEFM size effect, was revealed in previous tests of limited scope reported by Şener (1992, 1993) and Şener and Timur (1993).

The purpose of the present study is to report on a broader, more systematic study of the failure of bond splices in reinforced concrete beams subjected to bending and shear. As will be seen, the size effect in this type of failure is significant. Furthermore, the current and previous specifications of the ACI building code will be critically examined with respect to the size effect.

In contrast to Şener's (1993) previous studies, the splice failures are studied here on beams in flexure rather than bars in tension. Beam tests are easier to carry out and are more directly relevant to practical situations. However, a precise interpretation in terms of fracture mechanics becomes more difficult and has to be relegated to further study.

CURRENT CODE SPECIFICATIONS AND AVAILABLE FORMULAS

The size effect is understood as the dependence of the nominal strength of a structure on its size. The nominal bond strength in a splice may be defined as

$$\mu = \frac{T}{\pi d_b L_d} \qquad (1)$$

where T = tensile force in the bar, transmitted by the splice (in MN) calculated from the applied load according to the equilibrium equation

$$T = \frac{P_u a}{2\left[d - \frac{1}{2}(0.85c)\right]} \qquad (2)$$

Here, d_b = nominal diameter of the reinforcing bars (in mm); L_d = length of the bond splice (in mm); d = depth to the centroid of reinforcement (in mm) (Fig. 1); c = distance (in mm) from the compression face to the neutral axis, obtained by the standard equilibrium analysis of the cross section subjected to the bending moment; P_u = maximum (ultimate) load (in MN) that the beam can carry (Fig. 1); and a = shear span = moment arm of applied load (in mm) (Fig. 1).

The adequate strength of a lap splice is, in the ACI code, ensured by a provision that specifies the minimum length L_d of the lap of deformed bars to be proportional to the development length l_d of the bars (more precisely, $L_d = l_d$ if less than one-half of all the bars are spliced in the same cross section, and $L_d = 1.3l_d$ otherwise; see article 12.15.1 in standard ACI 318-95). The development length, in turn, is specified in the ACI building code as proportional to the bar diameter, d_b

$$l_d = d_b/k_d \qquad (3)$$

but always $l_d \geq 305$ mm (1 ft). Article 12.2.3 of the standard ACI 318-95 (''Building'' 1995) gives for l_d a formula equivalent to the expressions
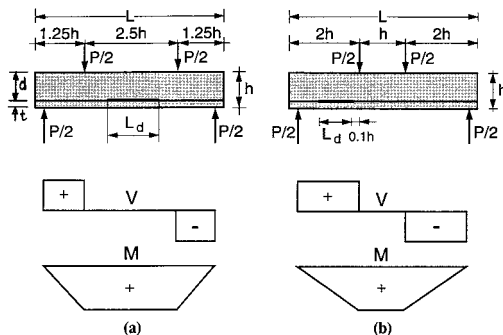

FIG. 1. Splice Locations, Loading, and Distributions of Shear Force *V* and Bending Moment *M*

$$k_d = \frac{20\sqrt{f_c'}\kappa}{\gamma(d_b)\alpha_l\beta_c\lambda_i f_y}; \quad \kappa = \frac{t + K_{tr}}{1.5\,d_b} \leq \frac{5}{3}; \quad K_{tr} = \frac{A_{tr}f_y}{1,500sn} \qquad (4)$$

Here, f_c' = standard compression strength of concrete; and f_y = yield strength of steel. Both are given in psi; l_d is in inches. The factor α_l accounts for the bar location, β_c for coating, and λ_i for concrete type (lightweight or not). Factor γ, depending on the reinforcement size (bar diameter), introduces a sort of discontinuous size effect; $\gamma(d_b) = 0.8$ for $d_b \leq 19.1$ mm (0.75 in., bar number 6), $\gamma(d_b) = 1$ for number 7 and larger bars. Furthermore, t = smallest of three values—cover on the side, cover over the bar, and one-half of the center-to-center bar spacing (in inches). A_{tr} = cross-sectional area of transverse steel (sq. in.); s = spacing of transverse reinforcement (in inches); and n = number of transverse bars or wires traversing a potential splitting plane.

The standard ACI 318-95 also gives an alternative simpler expression (article 12.2.2)

$$k_d = \frac{20\sqrt{f_c'}}{\alpha_l\beta_c\lambda_i f_y} \qquad (5)$$

which is valid when the bar spacing and the cover thickness are not less than d_b (otherwise, factor 20 is replaced with 40/3). Both (4) and (5) are equivalent when $\kappa = \gamma(d_b)$. For cover thickness $t = 19.05$ mm (0.75 in.) and $K_{tr} = 0$ (no confinement), this equivalence occurs when $d_b = 15.88$ mm (0.625 in.), i.e., for bars number 6.

The development length is defined as the length of the bar needed to transmit the yield force of the bar, i.e., $T = \pi d_b l_d \mu = f_y\pi d_b^2/4$, to the concrete. Solving for μ, we obtain the expression for the nominal bond strength in the splice according to ACI 318-95

$$\mu = (f_y/4)(d_b/l_d) = (f_y/4)k_d \qquad (6)$$

Later we will comment on the sudden major change made in the ACI specifications in 1995. The previous standard ACI 318-89 (''Building'' 1992) or ACI 318R-89, the 1992 revised standard (''Building'' 1992), (as well as the 1977 standard ACI 318-77 and the 1983 standard ACI 318-83) specified the formula $l_d = C_{mod}l_{bd}$, where C_{mod} is a modification factor depending on parameters (such as the cover thickness and bar spacing) other than the size (see sections 12.2.3–12.2.5 of ACI 318R-89, ''Building'' 1992), and $l_{bd} = \delta(d_b)f_y/\sqrt{f_c'}$ is the basic development length. In ACI 318R-89, $\delta(d_b) = 0.04A_b$ for a number 11 bar (or smaller), $\delta(d_b) = 0.085$ for a number 14 bar, and $\delta(d_b) = 0.125$ for a number 18 bar with $A_b = \pi d_b^2/4$ = cross-sectional area of the bar (see section 12.2.2 of ACI 318R-89). Using again $\mu = (f_y/4)(d_b/l_d)$, we see that the development length specification of the previous code ACI 318R-89 implied the nominal bond strength to be

$$\mu = \frac{\sqrt{f_c'}}{4}\frac{d_b}{C_{mod}\delta(d_b)} \qquad (7)$$

Applying statistical regression to the results of a large number of previously performed splice tests, Orangun et al. (1977) developed the following approximate empirical formula:

$$\mu_1 = \left(0.1 + 0.265\frac{t}{d_b} + 4.344\frac{d_b}{L_d} + 0.0025\frac{A_{tr}f_{yt}}{sd_b}\right)\sqrt{f_c'} \qquad (8)$$

exhibiting no size effect. Here μ_1 = nominal bond strength at age 28 d (in MPa); f_c' = standard cylindrical compression strength of concrete (in MPa); t = minimum thickness of concrete cover of the reinforcing bars (in mm); A_{tr} = combined cross-sectional area (in mm^2) of all reinforcements transverse to the splitting plane of the splice (i.e., crossing this plane perpendicularly); and f_{yt}, s = yield strength and spacing of the traversing reinforcement (in MPa and mm). For geometrically

similar structures, the ratios t/d_b, d_b/L_d, and A_{tr}/sd_b are constant, and so Orangun et al.'s formula exhibits no size effect.

Another useful formula is that of Zsutty (1985), also exhibiting no size effect

$$\mu_1 = 26.7f_c^{1/3} \left(\frac{d_b}{L_d}\right)^{1/2} \left(\frac{t}{d_b} + 2r\right)^{1/2}; \quad r = 100 \frac{A_{tr}}{sd_b} \qquad (9)$$

Here, r = steel ratio of the bars traversing the failure cross section. Since both formulas are approximate and give similar results, we will consider for size effect generalization only Orangun et al.'s formula. However, the type of generalization that follows could also be applied to Zsutty's formula.

APPLICATION OF SIZE EFFECT LAW

For generalization to the size effect, Orangun et al.'s formula is selected because, unlike the formula of ACI 318-95, whose plot will be shown later, it is smooth, with no discontinuities and, except for the size effect, has been better justified experimentally. It has served as the basis for the ACI 318 equations for the last several editions. The size effect correction can be approximately introduced into this formula according to the approximate size effect law of Bažant (1984). Since the test data to be studied suggest the existence of a nonzero residual nominal bond strength $\mu_r = \alpha_r\mu_1$ associated with a frictional-plastic mechanism, the extended form of the size effect law proposed by Bažant (1987) will be used. According to this law, the formula of Orangun et al. should be modified by a size-dependent multiplier as follows:

$$\mu = \mu_1 \left(\frac{\alpha_1}{\sqrt{1 + \beta}} + \alpha_r\right) \qquad (10)$$

in which

$$\beta = \frac{d}{d_0}; \quad \beta_1 = \frac{d_1}{d_0}; \quad \alpha_1 = (1 - \alpha_r)\sqrt{(1 + \beta_1)} \qquad (11)$$

In this formula, which is suggested as a possible form of a design formula, μ_1 = nominal bond strength of the splice given by (8) for a certain reference size $d = d_1$ to be determined empirically; μ = size-corrected nominal bond strength of the splice; β = relative size of the beam; d = characteristic size (dimension) of geometrically similar beams, which is taken here as the depth to the centroid of reinforcement (Fig. 1); and α_r = residual strength fraction = ratio of the residual nominal bond strength $\alpha_r\mu_1$ (for $d \to \infty$) to the nominal bond strength μ for reference size $d = d_1$. Eq. (10) gives the same result as (8) ($\mu = \mu_1$) for $d = d_1$, but not for other sizes of d.

The size effect is, in (10), characterized by three constants, d_0, d_1, and α_r, which can be determined from tests by regression. A theoretical determination of these constants may be possible, too, but it would require a difficult fracture mechanics analysis or nonlocal damage analysis.

TEST SPECIMENS AND EXPERIMENTAL METHOD

To study the size effect, geometrically similar beams of different sizes, containing lap splices of reinforcing bars, were tested at Gazi University, Ankara, Turkey (Fig. 1). The beams were similar in three dimensions, which means that the beam width b, cover thickness t, bar diameter d_b, and depth to reinforcement d were all proportional to the beam span L. The cross sections of all of the beams were square.

The bond splices were placed at two locations: (1) in the middle of a long midspan region with a uniform bending moment, which was achieved by applying two symmetric concentrated loads farther from midspan [Fig. 1(a)]; and (2) in a long end region of the beam with a uniform shear force (and a variable bending moment), which was achieved by applying

two symmetric concentrated loads closer to midspan [Fig. 1(b)]. In all of the specimens, the splices for the case of a uniform bending moment were centered at midspan. For the case of a uniform shear force, the splices were located at distance $0.1h$ from the concentrated loads. Each beam contained two longitudinal bars, which were both spliced in the same cross section. Although undesirable for design, this has been done in order to simplify the evaluation of the tests.

Three specimen sizes, characterized by beam heights of h = 50, 100, and 200 mm, were used. For all of the beams, the ratio of the span to the depth to reinforcement was $l/d = 6$ (Fig. 2), and the length-to-height ratio was $L/h = 5$. Three identical specimens were cast for each size and each type of splice. The test specimens with a uniform bending moment in the splice region (Fig. 2) as well as those with a uniform shear force (and a variable bending moment) in the splice region (Fig. 3) were geometrically similar in three dimensions. For the beams with splices in the end region, the shear span of all of the beams was $a = 2.3d$. For the beams with splices at midspan, the shear span of all of the beams was $a = 1.3d$.

The concrete mix proportions of water:cement:aggregate were 0.7:1:4 (by weight). All of the specimens, of all the sizes and types, were cast from the same batch of concrete in order to minimize statistical scatter of the results. Normal portland cement (NPC35, according to Turkish standard 19), similar to ASTM type I, and Kizilirmak River aggregate were used. The maximum aggregate size for all of the beams was $d_a = 4.76$ mm, which means that the concrete was a microconcrete. The use of a reduced aggregate size was necessary to obtain specimen dimensions that could be handled with the laboratory equipment available.

The specimens were subjected to moist curing for 21 d at room temperature. After that, they were exposed to a drying environment of relative humidity 50% and room temperature. They were tested at 28 d in a closed-loop testing machine (of stiffness constant 1.6 MN/mm), under a constant stroke rate. The stroke rate was selected so as to achieve the maximum load for each specimen within about 2 min.

Smooth (undeformed) reinforcing bars of yield strength 220 MPa, with diameters $\phi = 2$, 4, and 8 mm scaled in proportion to the beam size, were used (Fig. 2). To maintain geometric similarity, the cover thicknesses t were also scaled, and were 10, 20, and 40 mm. The reinforcement ratio was 0.31%. The lengths L_d of the bond splices of the steel bars were scaled, too. They were 27.5, 55, and 110 mm for the case of a uniform bending moment, and 30, 60, and 120 for the case of a uniform shear force. These lengths were selected to be less than the development length l_d required by ACI 318R-89, in order to prevent the steel bars from yielding before reaching the load that causes pullout failure of the splice.

Using a length of lap shorter than the development length of the bars is necessary for the splice to fail before the overall failure of the beams, i.e., to ensure that the maximum load will be controlled by splice failure and not by a bending or shear failure of the beam as a whole. The development length in actual design is larger because it must provide adequate safety against bond failure in the splice. But the adequacy of the safety margin cannot be ascertained without measuring the failure strength of the splice. This consideration justifies reducing the lapped length.

A reduced lap length of the splice might be thought to favor pullout of a bar from a smooth hole in concrete, which might be thought to be a phenomenon of plastic slip free of size effect. In reality, however, there is no plastic slip at the interface. The final breakage of bond on a smooth bar occurs by means of propagation of an interface cohesive crack between steel and concrete. The length of cohesive zone of this crack (which, doubtless, involves microcracking around the bar) is
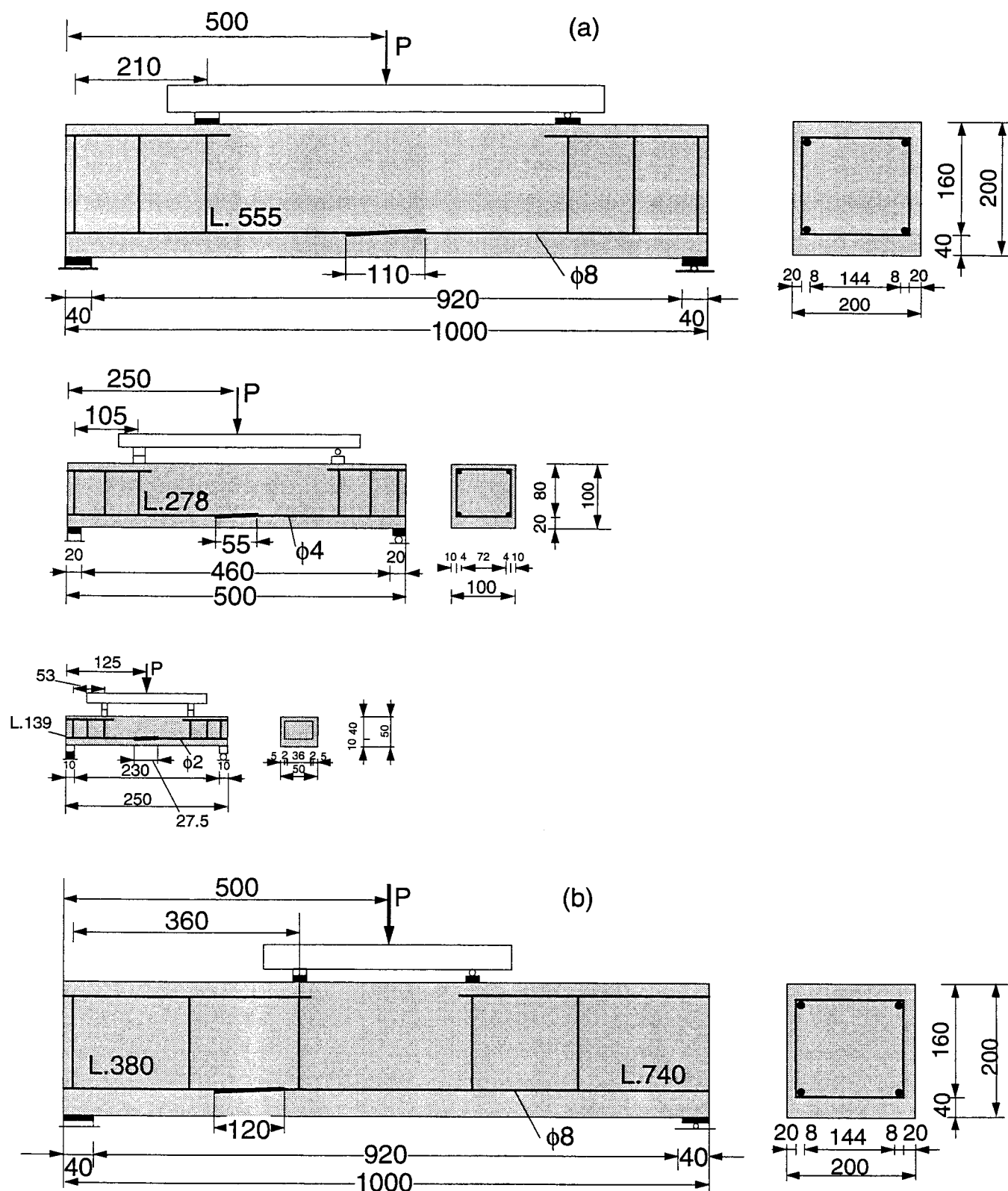
FIG. 2. Test Beams with Splices in: (a) Maximum Bending Moment Region (All Three Sizes Are Shown); (b) Maximum Shear Force Region (Only Largest Size is Shown)

more localized in larger bars relative to lap length, and thus to bar size. This causes a pronounced size effect even if there is no cracking around the bar (Bažant and Desmorat 1994; Bažant et al. 1995). In the present tests, however, cracking was always observed around the splice. Separation of the effects of the two phenomena, i.e., the crack propagation with distributed cracking around the bar and the interface crack

propagation, is impossible because they both cause a size effect.

Normally the lapped splices embedded in concrete are wrapped with wire, as used in previous tests by Şener (1993, 1994). To achieve a stronger confinement of concrete in the splice zone, precisely shaped wire spirals were installed around the lapped bars in one-half of the beams, and the other
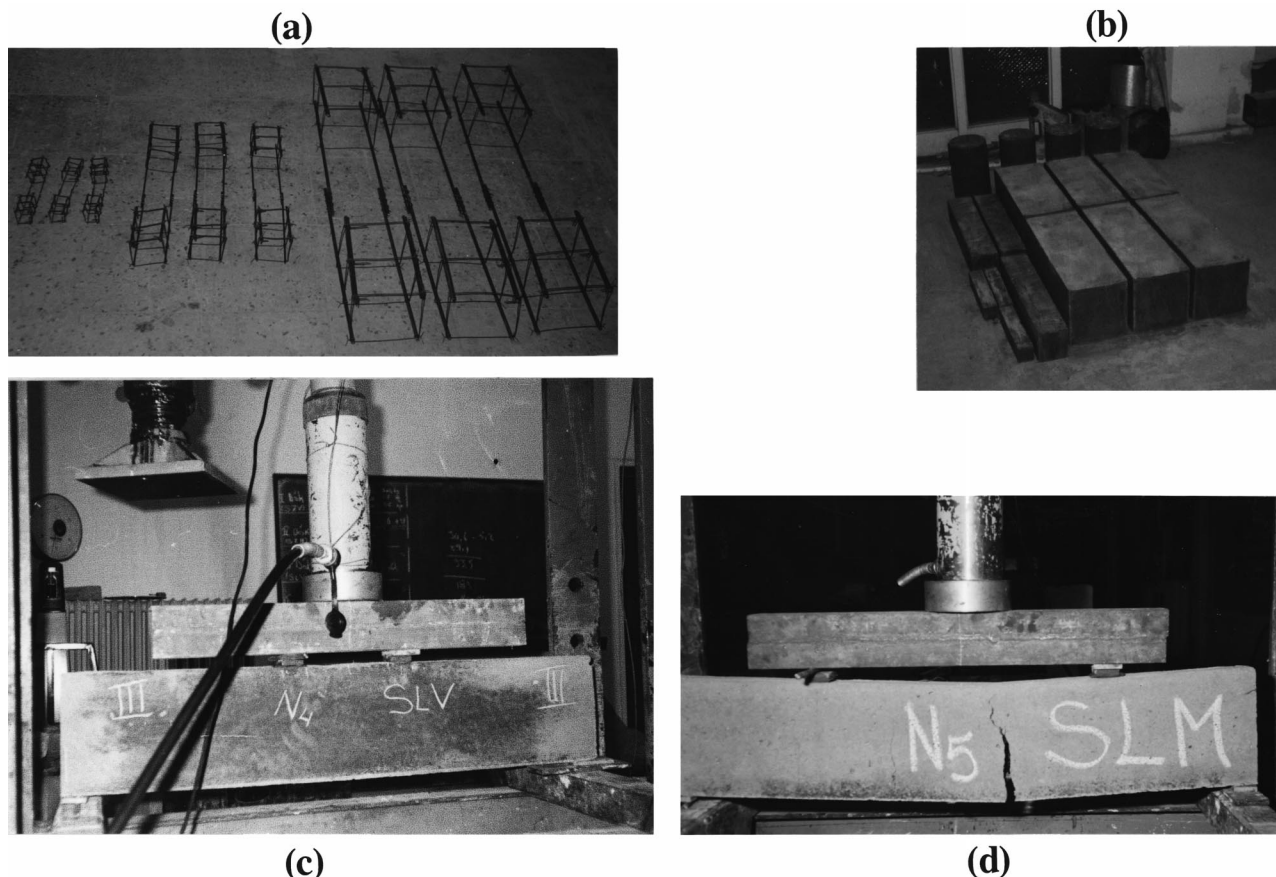
FIG. 3. Photo of: (a) Reinforcements for Beams with Splices at Midspan; (b) Beams before Testing; (c) Test Setup for Beam with Splice near Support; (d) Typical Failure of Beam with Splice at Midspan

half of the beams had no wire spiral. The diameters and lengths of the wire spirals were scaled in proportion to the bar sizes; the diameters were $\phi_s = 0.5$, 1, and 2 mm, and the lengths were 37.7, 75.4, and 150.8 mm. The spirals had three pitches. The height of the pitches for the small, medium, and large bars was 12.5, 25, and 50 mm, respectively. For each size and splice location, three beams with spirals and three without spirals were tested. This made a total of $3 \times 3 \times 2 = 18$ beams with spirals, and 18 without spirals.

The typical mode of failure of a beam with a splice in the midspan region is seen in Fig. 3(d).

TEST RESULTS AND THEIR ANALYSIS

The splices failed in two different modes. One mode was a splitting of concrete along the bars (labeled SP in Table 1), and the other was pullout (PO) of the bar with a transverse crack initiating at the end of the steel bar. For beams with splices at midspan, one large vertical crack developed, as seen in Fig. 3(d). For beams with splices near the support, cracks started vertically and one of them propagated in an inclined direction toward the load. The postpeak load-deflection diagrams for larger beams were steeper than those for smaller beams, confirming an increase of brittleness of response with increasing size. This is similar to the behavior observed previously at Northwestern University in tests of punching shear, torsion, and pullout (''Fracture'' 1992; Bažant et al. 1994).

Both splices in the beam appeared to fail simultaneously. This would not be expected, for stability reasons, if the failure zone in the splice were extremely localized. However, since the cracking and fractures around the splice were spread over a large zone, a simultaneous failure of both nearby splices is a reasonable assumption for the evaluation of test results.

For the purpose of statistical regression of test data, (10) is better rewritten as

$$\mu = \mu_0 \left(\frac{1}{\sqrt{1 + \beta}} + \alpha_R \right) \tag{12}$$

where

$$\mu_0 = \mu_1 \alpha_1; \quad \alpha_R = \alpha_r / \alpha_1 \tag{13}$$

The reference size has been chosen as the depth to reinforcement $d_1 = 83.3$ mm (which corresponds to beam height $h = 100$ mm). The unknown constants μ_0, d_0, and α_R in (12) can be determined by iterating linear statistical regressions of the measured maximum loads P_u, which are listed in Table 1. A linear regression can be achieved by rearranging (12) as follows:

$$Y = AX + C \tag{14}$$

in which

$$X = d; \quad Y = (\mu - \alpha_R \mu_0)^{-2} \tag{15}$$

$$A = C/d_0; \quad C = \mu_0^{-2} \tag{16}$$

First, one must select a series of many values of α_R (between 0 and 1, e.g., $\alpha_R = 0$, 0.001, 0.002, 0.003, ... 0.999, 1). Then, for each of them, one runs a computer fitting of the test data by linear regression in the plot of Y versus X, and calculates the correlation coefficient r of the regression. Finally, one selects the regression for which the value of r is the highest. For each α_R value, the procedure is analogous to that described in the Reunion Internationale des Laboratoires d'Essais et de Recherches sur les Matériaux et les Constructions (RILEM) recommendation (Bažant 1990). For the values of A and C thus obtained, (16) can be solved to provide $d_0 = C/A$ and $\mu_0 = 1/\sqrt{C}$. Then, according to (11)

TABLE 1. Measured Maximum Loads P_u

Beam number (1)	t (mm) (2)	d_b (mm) (3)	L_d (mm) (4)	f'_c (MPa) (5)	P_u (N) (6)	T (N) (7)	μ (MPa) (8)	Failure mode (9)
A1	40	8	110	24.5	36,500	24,064	8.70	SP
A2	40	8	110	24.5	42,000	27,691	10.02	SP
A3	40	8	110	24.5	40,000	26,372	9.54	SP
A4	20	4	55	24.5	9,800	6,461	9.35	PO
A5	20	4	55	24.5	11,000	7,252	10.49	PO
A6	20	4	55	24.5	10,100	6,659	9.63	PO
A7	10	2	27.5	24.5	3,000	1,978	11.45	PO
A8	10	2	27.5	24.5	3,000	1,978	11.45	PO
A9	10	2	27.5	24.5	3,150	2,077	12.02	PO
B1	40	8	110	25	40,000	26,364	9.54	SP
B2	40	8	110	25	43,000	28,342	10.25	SP
B3	40	8	110	25	46,000	30,319	10.97	SP
B4	20	4	55	25	11,000	7,250	10.49	PO
B5	20	4	55	25	11,500	7,580	10.97	PO
B6	20	4	55	25	10,500	6,921	10.01	PO
B7	10	2	27.5	25	3,300	2,175	12.59	PO
B8	10	2	27.5	25	3,200	2,109	12.21	PO
B9	10	2	27.5	25	3,250	2,142	12.40	PO
C1	40	8	120	26.6	26,000	30,294	10.04	SP
C2	40	8	120	26.6	29,000	33,789	11.20	SP
C3	40	8	120	26.6	26,300	30,643	10.16	SP
C4	20	4	60	26.6	8,150	9,496	12.59	PO
C5	20	4	60	26.6	7,850	9,146	12.13	PO
C6	20	4	60	26.6	7,250	8,447	11.20	PO
C7	10	2	30	26.6	3,450	4,020	21.33	PO
C8	10	2	30	26.6	3,000	3,495	18.54	PO
C9	10	2	30	26.6	2,850	3,321	17.62	PO
D1	40	8	120	26.4	26,450	30,821	10.22	SP
D2	40	8	120	26.4	30,950	36,065	11.96	SP
D3	40	8	120	26.4	32,000	37,288	12.36	SP
D4	20	4	60	26.4	7,250	8,448	11.20	PO
D5	20	4	60	26.4	7,000	8,157	10.82	PO
D6	20	4	60	26.4	7,500	8,739	11.59	PO
D7	10	2	30	26.4	2,850	3,321	17.62	PO
D8	10	2	30	26.4	2,700	3,146	16.69	PO
D9	10	2	30	26.4	2,500	2,913	15.45	PO

$$\alpha_r = \frac{\alpha_R\sqrt{1 + \beta_1}}{1 + \alpha_R\sqrt{1 + \beta_1}}; \quad \mu_1 = \frac{\mu_0}{(1 - \alpha_r)\sqrt{1 + \beta_1}} \quad (17)$$

where d_1 = chosen reference size.

Another way to identify μ_1, d_0, and α_r is to apply the standard library subroutine for the Marquardt-Levenberg nonlinear optimization algorithm. The optimization uses (12), and determines α_r and μ_1 from the following relations:

$$\mu_1 = \mu_0\left(\frac{1}{\sqrt{1 + \beta_1}} + \alpha_R\right) \quad (18)$$

and

$$\alpha_r = \frac{\alpha_R\sqrt{1 + \beta_1}}{1 + \alpha_R\sqrt{1 + \beta_1}} \quad (19)$$

This second method was selected in the present analysis. The calculated values of μ_0, d_0, μ_1, and α_R are indicated in Table 2.

Note that parameter d_0, representing the transitional size between nonbrittle and brittle behaviors, has the geometrical meaning of the intersection of the horizontal asymptote (corresponding to the strength theory) and the inclined asymptote (corresponding to LEFM). In all tests, d_0 is rather small in comparison to the maximum aggregate size d_a. Indeed, d_0 is of the order of 1 mm for the bending tests, and 1.80 mm for the shear tests. These values are about 20% and 40% of the maximum aggregate size ($d_a = 4.76$ mm), respectively. On average, d_0 is about 30% of the maximum aggregate size. However, further tests are needed to improve this estimate because the value of d_0 seems to depend strongly on the type of test performed. For the same reason, the brittleness of splice failure seems to depend as well on the type of test performed.

In the case of bending tests, the positive curvature of the trend of the data points in the doubly logarithmic size effect plots suggests a finite residual strength in extrapolation to infinite size. Indeed, the optimal value of α_R is found to be 0.25, which corresponds to a residual strength $\mu_r = 0.2\mu_{max}$ (where $\mu_r = \alpha_r\mu_1$). The curves have similar shapes in both cases (without and with spirals), and the data points are located in the part of the plot with positive curvature. Also, the maximum and residual bond strength values are of the same order of magnitude, with slightly higher values in the bending test with spirals. Therefore, the spirals do not significantly increase the bond strength of the bending specimen. The slope of the curve was computed at $x = 80$ mm in both cases. In Figs. 4 and 5, this slope is seen to be much smaller than the LEFM slope; the r values of the slope are about -15% (as reported in Table 2). Therefore, the failure of the splices in bending tests is less brittle compared to the linear elastic theory, and the spirals do not play a significant role in reducing the brittleness of the failure in this type of test.

In the case of the shear tests, the maximum strengths are significantly higher than those for the bending tests (Table 2). On the other hand, the residual strengths are smaller or even negligible. Indeed, in the case of the shear test without spirals, there is no residual strength (i.e., $\alpha_R = 0$, which corresponds to infinite size). When spirals are added, the residual strength represents only 10% of μ_0. Again, the slopes were computed at $x = 80$ mm. For the shear test with spirals, the slope is twice as high as that for the bending tests, as shown in Table 2. As can be seen in Fig. 6, the behavior of the specimen in shear tests without spirals is close to that predicted by LEFM.

Therefore, one can conclude that the bond fracture of the specimen depends on the type of test performed, and that it is more brittle in a shear test than in a bending test. However, in the case of shear, the spirals reduce significantly the brittleness of fracture under shear, as seen upon comparing the slopes of the curves in Figs. 6 and 7. This may have been expected because the splice failure is not just a failure of the splice (which includes propagation of frictional interface shear cracks between steel and concrete and microcracking around the splice), but also a failure of the cross section as a whole. For the splices at midspan, there is a major vertical crack [Fig. 3(d)] and the overall failure is of flexure type, whereas for the splices near the support, there is a major inclined crack and the failure mode is akin to diagonal shear, which is known to be much more brittle than bending. These failure modes also significantly differ from the splice failures in tensioned bars [which were tested by Şener (1994)].

TABLE 2. Parameters' Calculated Values

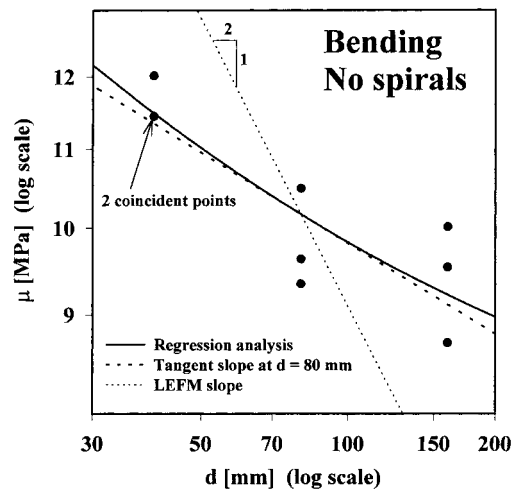| Test (1)	α_R (2)	μ_0 (3)	d_0 (4)	β_1 (mm) (5)	μ_1 (6)	α_r (7)	μ_{max} (8)	μ_r (9)	Slope at $x = 80$ mm (10)
Bending	0.25	27.64	1.13	73.72	10.11	0.68	34.55	6.91	−0.158
Bending with spirals	0.25	31.03	0.84	98.88	10.86	0.71	38.78	7.76	−0.14
Shear	0	58.81	1.9	43.85	8.78	0	58.81	0	−0.455
Shear with spirals	0.1	52.36	1.72	48.48	12.68	0.41	57.6	5.24	−0.29

FIG. 4. Measured Nominal Bond Strengths in Splices of Beams without Spirals in Maximum Moment Region (Based on Table 1, A1–A9), and Fit by Size Effect Formula
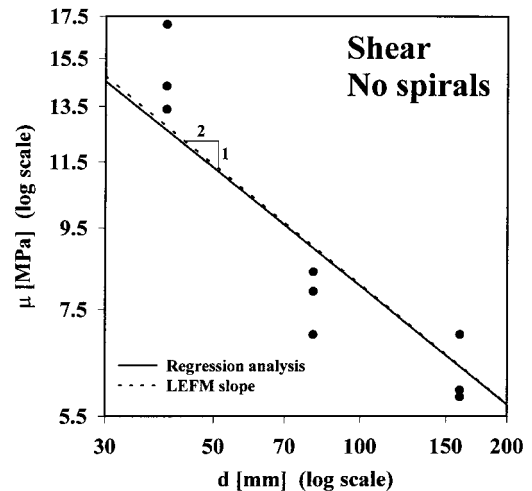

FIG. 6. Measured Nominal Bond Strengths in Splices in Beams with Wire-Wrapped Splices in Maximum Shear Force Region (Based on Table 1, C1–C9), and Fit by Size Effect Formula
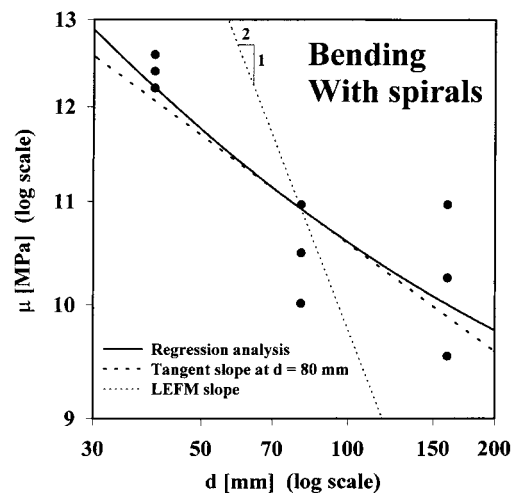

FIG. 5. Measured Nominal Bond Strengths in Splices of Beams with Splices Confined by Spirals in Maximum Moment Region (Based on Table 1, B1–B9), and Fit by Size Effect Formula
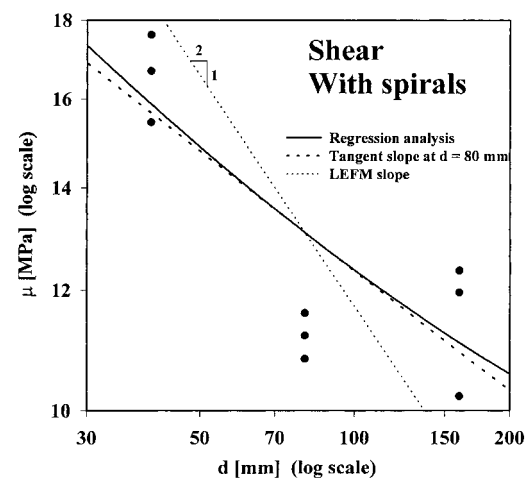

FIG. 7. Measured Nominal Bond Strengths in Splices of Beams with Splices without Spirals in Maximum Shear Force Region (Based on Table 1, D1–D9), and Fit by Size Effect Formula

The scope of the present tests unfortunately appears insufficient for proposing a good formula to predict d_0, d_1, and α_r from the characteristics of concrete. That will have to await more extensive testing with different types of concrete.

It is nevertheless apparent that d_0 for splices near the support is larger than that for splices at midspan, and that for splices without spirals it is somewhat larger than that for splices with spirals.

Because of these differences in the mode of failure for splices at different locations, it appears difficult to devise, at this time, a simple general formula for predicting the values of the transitional size d_0 in (10). Obviously, the splice failure is a rather complex type of brittle failure, with a size effect that is strongly correlated to the overall failure mode of the beam. Development of a practical formula for d_0 will necessitate further theoretical as well as experimental studies.

The reason why smooth bars had to be used was that deformed bars of sufficiently small diameters for these tests were unavailable. For deformed bars, the size effect might be expected to be less pronounced, but probably not much less because, even for smooth bars, the pullout and splice failures are caused mainly by fracturing of the concrete around the splice and not simply by slip along the interface.

Finally, it must be admitted that the present and preceding test results are still of a limited scope. Further tests should cover a broader range of sizes and other conditions. Especially needed are size effect tests for concretes with normal aggregate sizes.

COMMENTS ON ACI CODE SPECIFICATIONS

The curves of the size effect implied by the development length provisions of ACI 318-95 (for $\kappa = 2/3$) and ACI 318R-89 are plotted in logarithmic scales in Fig. 8. Because the size effect is defined only for geometrically similar structures, the plots are made under the assumption that κ is constant. If the value of κ is changed, the stepped curve of ACI 318-95 is merely shifted up or down as a rigid body. Although the plots in the figure extend up to bars number 18, note that the code prohibits bars larger than number 11 to be spliced by laps.

For ACI 318-95, the size effect is seen in Fig. 8 to exist only in the sudden jump between bars number 6 and 7. The jump is a simple way to handle the size effect. Such discontinuity is also undesirable from the viewpoint of optimization of design because it would spoil convergence of optimization subroutines if applied to design. It unreasonably penalizes bars number 7 compared to number 6. Comparing the change in μ between the left and right ends of the plot of ACI 318-95 provision in Fig. 8 to the LEFM slope $-1/2$, we see that the
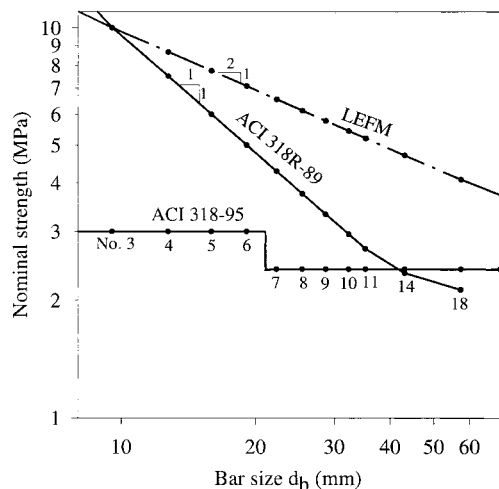
FIG. 8. Size Effect on Nominal Bond Strength Implied by Development Length Provisions of ACI Code

size effect in ACI 318-95 is far too weak. A revision is in order because, for the present test results, the overall slope is much closer to the LEFM slope (Figs. 4–7).

It is striking that the size effect implied by the development length provisions of the previous standard ACI 318-89 (also ACI 318-77 and ACI 318-83), i.e., $\mu \propto 1/d_b$, is so much stronger (it give the slope $-1/1$ in Fig. 8). The size effect is, in fact, twice as strong as that in LEFM, in which $\mu \propto \sqrt{d_b}$ (compared to the slope $-1/2$ for the LEFM size effect shown in Fig. 8). This is, however, caused by the fact that the previous code specification, resulting in (17), has been taken here beyond its intended purpose. It was not intended to be used for any cover thickness t other than the standard thickness, which is a constant. To judge the size effect, the cover thickness must be considered to be proportional to the bar diameter (i.e., d_b/t is constant for the curve in Fig. 8). But that goes beyond the original intention of the ACI code provision.

The sudden change from the unreasonably strong size effect that was implied, albeit indirectly, by the previous ACI specifications to the unreasonably weak size effect that is implied by the current specifications gives, nevertheless, the impression of a vacillation. The fact that such a sudden U-turn in the ACI specifications, evidenced in Fig. 8, was made in 1995 despite the absence of any revolutionary new findings invites doubt.

When, however, both the cover thickness t and the value of K_{tr} in the current ACI 318-95 are considered constant, the effect of bar size d_b on the nominal bond strength according to (4) is also of the type $\mu \propto 1/d_b$, and thus similar to ACI 318R-89. So, in that case, there is agreement.

Chapter 12 of ACI 318 does not allow smooth bars to be spliced, and all of its provisions refer specifically to deformed bars. However, to assume, on this basis, that the present conclusions about size effect based on tests of smooth bars do not apply at least approximately would be unreasonable.

CONCLUSIONS

1. Similar to previous investigations of other brittle failures of reinforced concrete structures, the present test results for the failure of beam splices of smooth bars clearly confirm the existence of a significant size effect on the nominal bond strength in the splice, accompanied by an increase of failure brittleness with the bar size. The size effect should therefore be introduced as a correction to the existing code specification.

2. Using a spiral surrounding the splice greatly reduces the size effect and diminishes the brittleness in bond failure.

3. The splice failure in the maximum shear force region of a beam exhibits a much stronger size effect and a much higher brittleness than the splice failure in the maximum moment region of a beam.

4. The development length provisions of the current standard ACI 318-95 imply a certain size effect on the nominal bond strength. However, the implied size effect, representing a discontinuous jump, is unreasonable, computationally undesirable, and much too weak.

5. On the other hand, the development length provisions of the previous standards ACI 318R-89, ACI 318-89, ACI 318-83, and ACI 318-77 implied an excessive size effect, twice as strong as the size effect in LEFM.

6. A simple improvement of an existing design formula by including a size effect multiplier is proposed. It should be used in design as a safer alternative appropriate for large structures. However, further testing is needed to obtain a solid experimental basis for further improvement of this formula.

APPENDIX.   REFERENCES

Bažant, Z. P. (1984). "Size effect in blunt fracture: Concrete, rock, metal." *J. Engrg. Mech.*, ASCE, 110(4), 518–535.

Bažant, Z. P. (1987). "Fracture energy of heterogeneous material and similitude." *SEM-RILEM Int. Conf. on Fracture of Concrete and Rock*, S. P. Shah and S. E. Swartz, eds., Society for Experimental Mechanics, 390–402.

Bažant, Z. P. (1990). "Size effect method for determining fracture energy and process zone of concrete." *Mat. and Struct.*, 23, 461–465.

Bažant, Z. P. (1995). "Scaling theories for quasibrittle fracture: Recent advances and new directions." *Fracture mechanics of concrete structures*, F. H. Wittmann, ed., Aedificatio, Freiburg, Germany, 515–534.

Bažant, Z. P., and Desmorat, R. (1994). "Size effect in fiber or bar pullout with interface softening slip." *J. Engrg. Mech.*, ASCE, 120(9), 1945–1962.

Bažant, Z. P., Li, Z., and Thoma, M. (1995). "Identification of stress-slip law for bar or fiber pullout by size effect tests." *J. Engrg. Mech.*, ASCE, 121(5), 620–625.

Bažant, Z. P., Ožbolt, J., and Eligehausen, R. (1994). "Fracture size effect: Review of evidence for concrete structures." *J. Struct. Engrg.*, ASCE, 120, 2377–2398.

Bažant, Z. P., and Planas, J. (1998). *Fracture and size effect in concrete and other quasibrittle materials*. CRC Press, Boca Raton, Fla.

Bažant, Z. P., and Şener, S. (1988). "Size effect in pullout tests." *ACI Mat. J.*, 85, 347–351.

"Building code requirements for reinforced concrete." (1992). *ACI 318R-89*. American Concrete Institute, Detroit.

"Building code requirements for reinforced concrete." (1995). *ACI 318-95*. American Concrete Institute, Detroit.

"Fracture mechanics of concrete: Concepts, models and determination of material properties." (1992). *Fracture mechanics of concrete structures*, Z. P. Bažant, ed., Elsevier Applied Science, London, 1–140.

Orangun, C. O., Jirsa, J. O., and Breen, J. E. (1977). "A reevaluation of test data on development length and splices." *ACI J.*, 74(3), 114–122.

Şener, S. (1992). "Size effect in bond splices tests." *FIP '92 Symp.*, G. Tassi, ed., Hungarian Scientific Society of Building, Budapest, 357–362.

Şener, S. (1993). "Size effect in the direct loading tests." *Advances in civil engineering. Proc., 1st Tech. Congr.*, Middle East Technical University, Ankara, Turkey, 720–727.

Şener, S. (1994). "Failure of steel bars in R. C. beams: Test of size effect." *Bull. of Tech. Univ. of Instanbul*, 47, 337–355.

Şener, S., and Timur, I. (1993). "Size effect in bond splices test under the indirect loading." *Advances in civil engineering. Proc., 1st Tech. Congr.*, Middle East Technical University, Ankara, Turkey, 728–735.

Zsutty, T. (1985). "Empirical study of bar development behavior." *J. Struct. Engrg.*, ASCE, 111(1), 205–219.